Adsorption of Malachite Green Oxalate Dye by CuCo$_2$O$_4$/MgO Spinel Oxide Nanocomposite

Tariq Hussein Mgheer[1], Ali Abdulraheem Kadhim[2*], Zainab Abdalameer Hussein[3], Zaid Kaheel Kadhim[4], Muneer Abdul Aly Al-Da'amy[5], Abbas Jassim Atiyah[6], Salih Hadi Kadhim[6], and Suma Jaafar Abbas[3]

[1]*Department of Chemistry and Biochemistry, College of Medicine, University of Babylon, Hilla 51002, Iraq*

[2]*Department of Animal Production, College of Agriculture, University of Kerbala, Karbala 56001, Iraq*

[3]*Department of Plant Protection, College of Agriculture, University of Kerbala, Karbala 56001, Iraq*

[4]*Department of Horticulture and Landscape, College of Agriculture, University of Kerbala, Karbala 56001, Iraq*

[5]*Department of Chemistry, College of Pure Science for Education, University of Kerbala, Karbala 56001, Iraq*

[6]*Department of Chemistry, College of Science, University of Babylon, Hilla 51002, Iraq*

Abstract: *The current study involves a synthesis of a composite of copper oxide and cobalt oxide as a spinel oxide load over magnesium oxide. This synthesis of nanocomposite material was from nitrate salts of the corresponding metals by co-precipitation method, while it was investigated by Fourier transform infrared spectroscopy (FTIR), X-ray diffraction techniques (XRD), field emission scanning electron microscopy (FESEM), atomic force microscopy (AFM), and the activity of these materials was estimated by appreciated adsorption of malachite green oxalate (MGO) dye from its aqueous solution. Adsorption isotherm was investigated using both Freundlich and Langmuir adsorption isotherms. While the results of the spectrophotometric studies showed that the composition of synthesized supported oxides at 450 °C was spinel type with nanoparticle size, and the optimum removal efficiency was around 98% for the adsorption of MGO dye over spinel nanocomposite surface achieved by using a dye concentration of 5 ppm, a mass of adsorbent surface of 5 mg, in terms of the adsorption model's isotherms the obtained results showed that the removal of MGO dye by the surface of this material was more fitted with the Freundlich models' adsorption.*

Keywords: *malachite green oxalate dye; CuCo$_2$O$_4$ spinel oxide; MgO; polluted dyes*

■ INTRODUCTION

Spinel structures that exist with transition metal oxides have attracted considerable attention to be used in many applications such as catalysis, photocatalysis, adsorption, and some pharmaceutical and medical applications [1]. Transition metal oxide spinel composites are characterized by abundant resources, low price, and biocompatibility. Due to all these factors, their manufacturers have recently become the research hot spot [2].

The electrocatalytic activities of composites metals oxides such as Ni$_3$O$_4$-Co$_3$O$_4$-Al$_2$O$_3$ and Co$_3$O$_4$·Fe$_3$O$_4$/CaO can be enhanced in comparison with their corresponding single metal oxides when the distribution of ions homogeneous in the respective lattice sites [3]. In this context, the captivation arrangement of the unfilled d-orbital electrons and the synergistic effect of both Cu and Co atoms in a unit cell of CuCo$_2$O$_4$ [4].

Despite the stability of metal oxides as catalysts, they have defects, including flocculation, toxicity, and

agglomeration [5]. Therefore, its properties were improved by adding other materials that act as carrier surfaces that can improve their physical and chemical properties with improving their catalytic activity [6]. There are also substances called emollients that can increase the efficiency of the catalyst. Important examples of these additives are calcium, zinc, and iron oxides [7].

Magnesium oxide used in this study is also considered a carrier surface on which cobalt and copper oxides are based [8]. The adsorption process is one of its important applications [9]. This probably arises from enhanced catalytic properties, including high BET surface area and moderate band gap [10].

The adsorption process is one of the best processes for removing toxic dyes from polluted environments, including air, water and soil [11]. Arora et al. used *Curcuma caesia*-based activated carbon to remove malachite green dye from an aqueous solution [12]. As well, Sharma et al. [13] used nanocomposite hydrogel for photocatalytic degradation of malachite green oxalate dye.

The present work aims to synthesize $CuCo_2O_4/MgO$ as a composite spinel-supported oxide and characterize a new adsorbent surface. The adsorption ability of the prepared material toward malachite green oxalate dye was investigated. This dye is chosen due to its wide use in the textile industries.

■ EXPERIMENTAL SECTION

Materials

The used chemicals were $Cu(NO_3)_2\cdot3H_2O$, $Mg(NO_3)_2\cdot6H_2O$, $Co(NO_3)_2\cdot6H_2O$, and Na_2CO_3 of high purity 99, 98 and 99 % respectively supplied from B.D.H company. Malachite green oxalate (MGO) dye ($C_{52}H_{54}N_4O_{12}$) was obtained from BDH Company. Fig. 1 showed the structural formula of the MGO dye [14].

Instrumentation

The experiments use several apparatuses including electronic balance TP-214 (Sartorius, Germany), UV-visible spectrophotometer double beam-6100PC (EMC LAB, Germany), muffle furnace size-two, oven Bs size two (Gallenkamp), ultrasonic set, and heater with magnetic
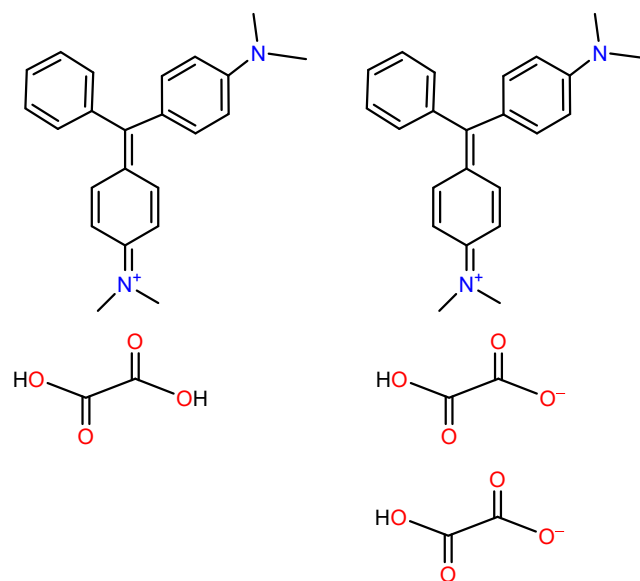

Fig 1. The structural formula of MGO

stir MR Hei-standard (Heldolph. Germany). Instruments used for characterization included X-Ray XRD-6000 and FTIR IRAffinity-1S (Shimadzu, Japan), field-emission scanning electron microscope (FE-SEM) Tescan Mira3 (French), and atomic force microscope (AFM)TT-2 (AFM Workshop, USA).

Procedure

Synthesis of composite spinel oxide

A spinel oxide of copper and cobalt was prepared by calcinating their carbonates through the coprecipitation method [15]. Sodium carbonate was used as a precipitation agent in two ratios of 0.4 (2.431 g) and 0.6 (5.82 g) from their aqueous nitrates, respectively, at a reaction temperature of 60–70 °C. Then, the precipitant was filtered and washed with deionized distilled water until pH = 7. Next, the precipitate was dried at 120 °C for 24 h. After that, it was calcinated at 450 °C for 4 h, following the preparation method described in the previous study [16]. Magnesium oxide was also prepared separately by precipitation method from its aqueous nitrate at the same conditions [17]. Then, the copper and cobalt oxides were loaded on magnesium oxide at a ratio of 0.4 of dual oxide to 0.6 of magnesium oxide and mixed very well in 100 mL of distilled water using ultrasound for 30 min. The homogeneous oxides were filtered and dried, then calcined at 450 °C for 4 h. This is a

Tariq Hussein Mgheer et al.

modification of the method used by Kadhim [17] for preparing CuCo₂O₄/MgO.

Study of conditions of optimization adsorption

A series of volumetric flasks of 25 mL capacity was taken containing a dye solution with a concentration of 8 ppm. A weight of 0.01 mg of the adsorbent was added to each volumetric flask and placed in a water shaker. The percentage of dye removal was measured every 10 min, for 120 min after separating the adsorbent surface from the solution and finding the absorbance of the solution. As for the weight of the adsorbent surface, a series of volumetric flasks of 25 mL capacity of 8 ppm dye solution were also taken, in addition to the different weights in the range of 0.0025–0.015 g of the adsorbent surface and finding the percentage of dye removal at the optimization time [18]. In the same way, the function experiments were carried out with acidity and ionic strength [19];

$$Re\% = \frac{C_i - C_e}{C_i} \times 100\% \tag{1}$$

$$Q_e = \frac{V(C_i - C_e)}{m} \tag{2}$$

whereas, $Re\%$ = the removal efficiency of dye, C_i = the initial concentration of the MGO dye (before adsorption), C_e = equilibrium concentration of the MGO dye (after adsorption), Q_e = the capacity of the adsorbate in mg g⁻¹, m = the weight of CuCo₂O₄/MgO in units of g, and V is the total volume of the adsorbate solution in units L.

Isothermal study for adsorption of MGO dye over CuCo₂O₄/MgO composite

A series of different initial concentrations in the range of 4–12 mg L⁻¹ of MGO dye to construct the calibration curve to use for determination of the residual concentration of dye after each of the operations of the removal process. This study was carried out at different temperatures 298, 318, and 338 K and found the adsorption capacity (Q_e) at the optimum conditions of adsorption to study the isothermal adsorption temperature for adsorption of dye according to Giles's classification using the prepared adsorbent surface by plotting between the adsorption capacity Q_e and C_e [20].

■ RESULTS AND DISCUSSION

Characterization of Synthesized Metal Oxides

Functional groups of the prepared material were investigated using FTIR spectrometry. The obtained results are presented in Fig. 2. From these spectra, it is clear that the vibrations of stretching metal-oxygen bonds appeared in a range of less than 1000 cm⁻¹. The peaks at 436, 550 and 667 cm⁻¹ have corresponded to the vibrations of stretching bonds of $Mg^{2+}-O^{2-}$, tetrahedral $Co^{3+}-O^{2-}$ and octahedral $Cu^{2+}-O^{2-}$, respectively. This indicates that the synthesized oxides are a spinel type CuCo₂O₄/MgO [16,21-22]. The peaks around 2400 cm⁻¹ are related to the rocking vibrations of the metal oxide bonds [23].
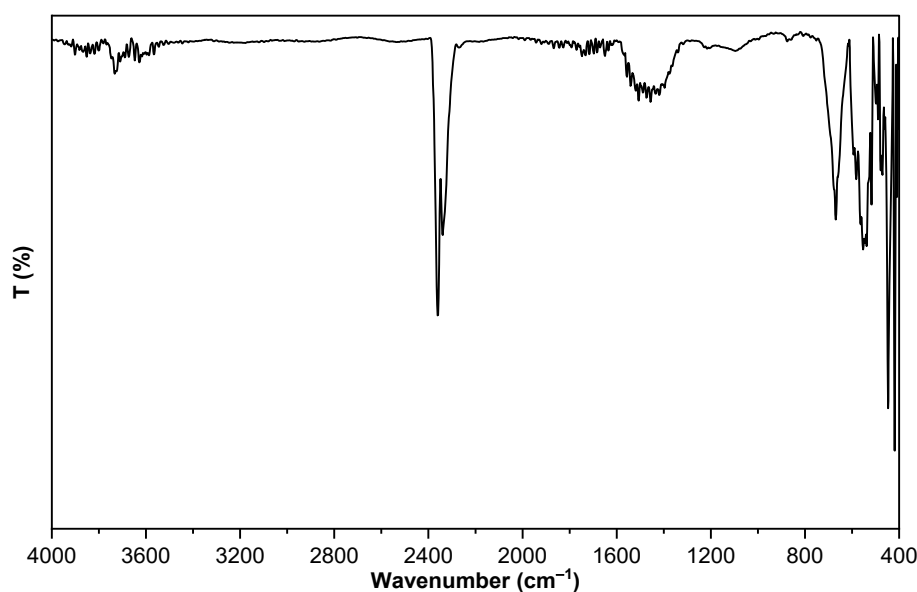

Fig 2. FTIR for Synthesized CuCo₂O₄/MgO

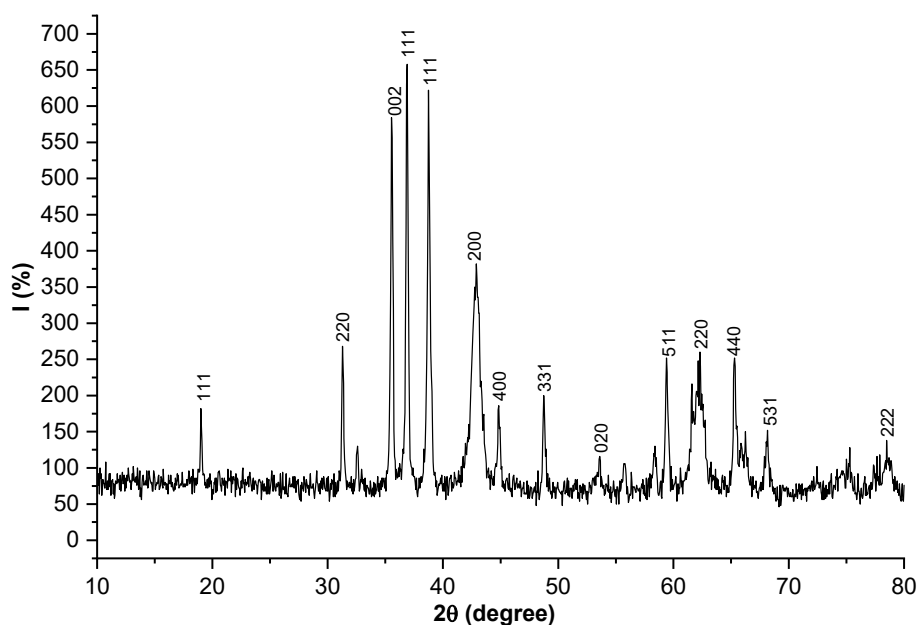**Fig 3.** XRD patterns for the synthesized CuCo₂O₄/MgO

The crystal structure of the prepared materials was investigated using X-ray diffraction patterns. These patterns are shown in Fig. 3; the main peaks at 2θ 19.03, 31.30, 32.58, 35.57, 36.89, 38.77, 42.93, 44.86, 48.76, 53.43, 55.74, 58.37, 59.41, 62.23, 65.29, 68.11 and 78.52 with Miller coefficients (111), (220), (110), (002), (111), (111), (200), (400), (331), (020), (422), (202), (511), (220), (440), (531), and (222), respectively, identical to the metal oxides of $CuCo_2O_4$ and MgO according to the standard JCPDS card for these materials [24-25].

The surface morphology of the synthesized material was screened using scanning electron microscopy, and the obtained image is presented in Fig. 4. From the obtained image, it can be seen that the presence of homogeneous flakes with an average particle size of around 33 nm, with the presence of spherical granules particles with an average size of around 27 nm, MgO and $CuCo_2O_4$.

AFM was also utilized in the investigation topography of the synthesized materials. The obtained results are presented in Fig. 5. AFM image showed a relative homogeneity of the surface's topography of these oxides and their roughness coefficient.

Optimization Conditions for Removal of MGO Dye by Adsorption over CuCo₂O₄/MgO Spinel Oxide

Fig. 6 shows the calibration curve of MGO dye, which was done for the determination of the dye concentration after each adsorption process.
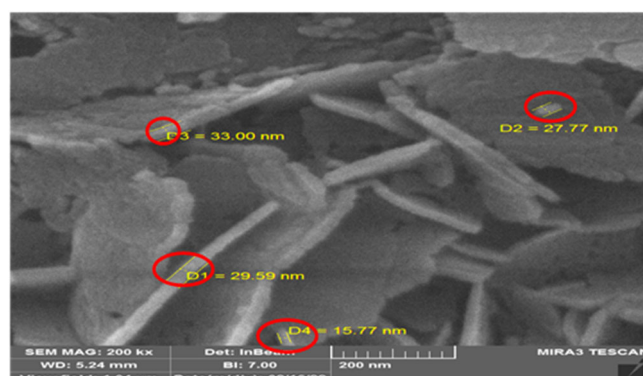

Fig 4. FESEM image for CuCo₂O₄/MgO spinel oxide

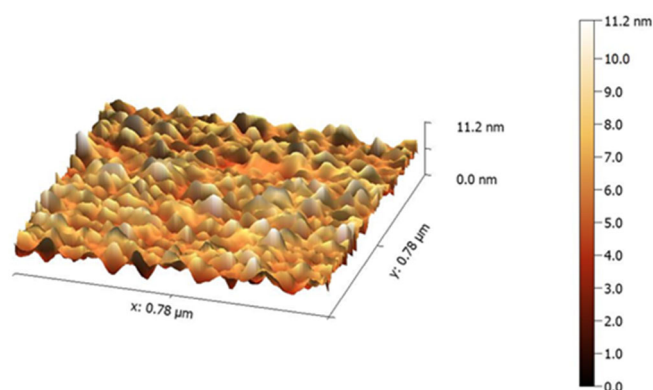**Fig 5.** AFM image for synthesized CuCo₂O₄/MgO spinel oxide

Contact time is one of the most important factors influencing the adsorption process, and it is the time required for adsorbent particles to stick to the adsorbent surface. From Fig. 7, we noticed a sudden increase in the removal rate in the first 10 min. Then it was increased to reach a high percentage after 50 min. After that, the removal rate remains almost constant for up to 120 min. As a result of the adhesion of all adsorbent particles to the adsorbed surface during the first 60 min. This observation arises from the gradual filling of active sites at the adsorbent surface with MGO dye molecules with time progress until it becomes fully saturated, which leads to reduce the rate of dye removal over the adsorbent surface [18].

Fig. 8 shows the effect of the adsorbent surface weight on the efficiency of dye removal. From these results, it can be seen that the adsorption capacity was increased with the increase of adsorbent surface weight because this can lead to an increased number of active sites on the adsorbent surface with the increase of the amount of adsorbent surface in the adsorption process [26].
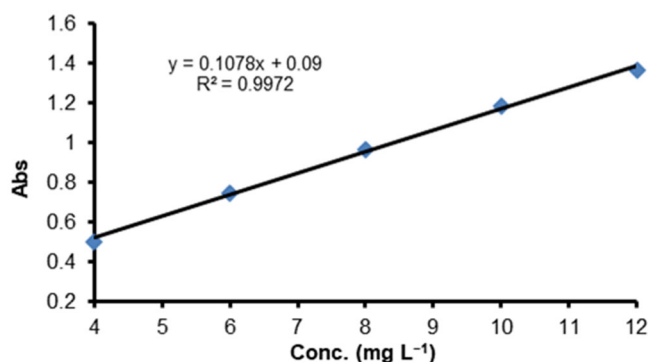
Fig. 9 shows the adsorption isotherm in which the relationship between the adsorption capacity of Q_e and C_e adsorbents when using different initial concentrations of 4–12 mg L^{-1} was, according to Giles S4 classification, the reason for the high-affinity adsorbents and surface adsorbents at 298–338 K [27].

Figs. 10, 11, and 12 show Freundlich, Langmuir, and Temkin adsorption isotherms; these were calculated according to Eq. (3–5). The values of constants for each of
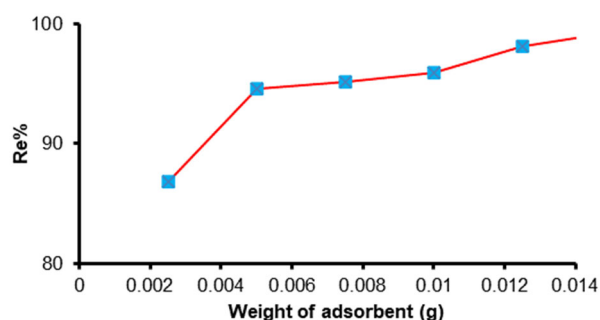
Fig 8. Effect of the weight of $CuCo_2O_4/MgO$ adsorbent surface on adsorption MGO dye

Fig 6. Calibration curve of MGO dye at wavelength 620 nm
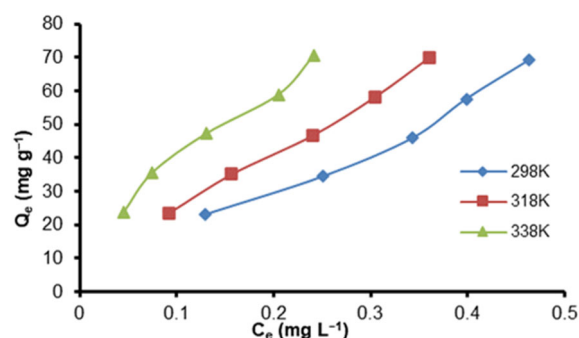
Fig 9. Isothermal of adsorption MGO dye over $CuCo_2O_4/MgO$ adsorbent surface at 298, 318, and 338 K

Fig 7. Contact time of MGO dye particles on $CuCo_2O_4/MgO$ adsorbent surface

Fig 10. Relationship between C_e/Q_e and C_e for MGO dye over $CuCo_2O_4/MgO$ adsorbent surface at 298, 318, and 338 K

Fig 11. Relationship between log Q_e and log C_e for MGO dye over $CuCo_2O_4/MgO$ adsorbent surface at 298, 318, and 338 K
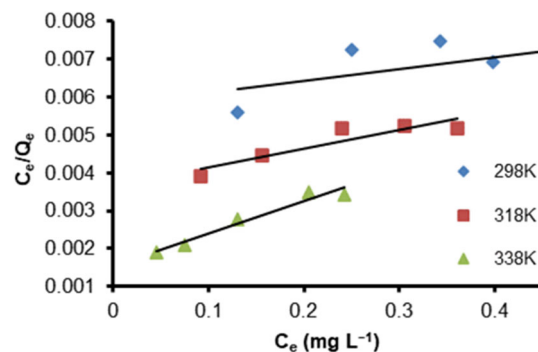

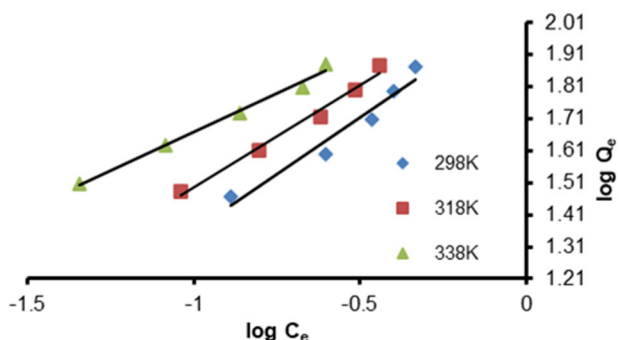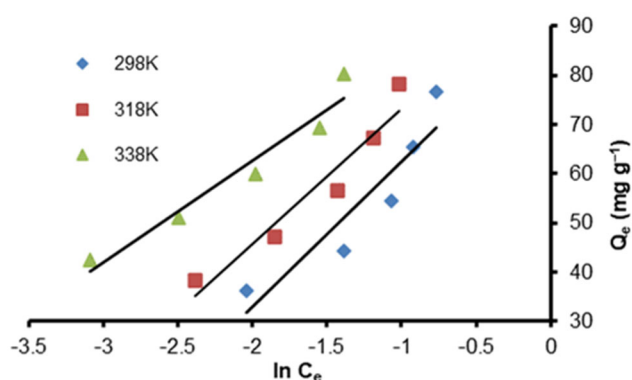**Fig 12.** Relationship between Q_e and ln C_e for MGO dye over $CuCo_2O_4/MgO$ adsorbent surface at 298, 318, and 338 K

the model's adsorption equations and all the results are summarized in Table 1. The adsorption process applies to Freundlich and Temkin equations while the Langmuir equation does not apply to Freundlich because Langmuir originally proposed that the adsorption process occurs on one layer after that, Freundlich and Temkin modified Langmuir's equation for the adsorption process occur in more than one layer [28-29];

$$Q_e = \frac{abC_e}{1+bC_e} \quad \text{Langmuir} \qquad (3)$$

where Q_e is adsorption gravimetric capacity in units (mg g^{-1}), C_e is the concentration of the solute adsorbent at equilibrium in units of mg L^{-1}, (a) best adsorption capacity when the adsorption surface is completely saturated in (mg g^{-1}) units, and b is Langmuir constant [30].

$$Q_e = k_f C_e^{1/n} \quad \text{Freundlich} \qquad (4)$$

The k_f and n are the experimental Freundlich constants while n and k_f are a measure of the intensity of adsorption and a measure of the amount of adsorption, respectively [30].

$$Q_e = \frac{RT}{b} LnA_T C_e \quad \text{Temkin} \qquad (5)$$

The A_T is the adsorption equilibrium constant representing the maximum adsorption energy while B is an enabling isotherm constant which is equal to RT/b (R: represents the general gas constant 8.314 J mol^{-1} K^{-1}, T represents the absolute temperature K, and b the adsorption heat constant J mol^{-1}) [30].

Study of Thermodynamic Functions (ΔG, ΔH and ΔS)

The effect of temperature on the efficiency of MGO dye removal by adsorption over the prepared materials was studied, and thermodynamic functions (free energy ΔG, enthalpy ΔH, entropy ΔS) for the importance of this conception to the adsorption process and determining the type of reaction spontaneous or not, exothermic or endothermic [33]. The free energy ΔG was calculated using Eq. (10), while ΔH was calculated by sketching the relationship between the equilibrium constant ln K_{eq}, which is shown in Fig. 13 and Table 2. From the negative value of ΔG, it appears that the adsorption process occurs spontaneously and does not need energy. The heat of the reaction is positive, indicating that the adsorption process is an endothermic process, while the

Table 1. Langmuir, Freundlich, and Temkin constants and correlation coefficient for adsorption of MGO dye over $CuCo_2O_4/MgO$

Temperature	Langmuir isotherm			Freundlich isotherm			Temkin isotherm		
K	a	b	R^2	K_f	n	R^2	b_T	K_T	R^2
298	333.33	0.51	0.29	116.76	1.41	0.94	29.51	22.51	0.84
318	204.08	1.32	0.83	136.45	1.55	0.98	27.48	39.04	0.92
338	117.64	5.31	0.95	140.34	2.08	0.99	20.60	154.70	0.94

Table 2. Comparative Langmuir, Freundlich, and Temkin constants and correlation coefficient for adsorption of MGO dye

Adsorbent	Langmuir isotherm			Freundlich isotherm			Temkin isotherm			Ref.
	a	b	R^2	K_f	n	R^2	b_T	K_T	R^2	
SnO_2–NP–AC	142.87	2.33	0.9990	76.17	4.98	0.8320	19.91	63.00	0.8750	[31]
TLN	425.63	0.01	0.9528	42.57	3.19	0.9077	23.30	1.17	0.8997	[32]
$CuCo_2O_4/MgO$	333.33	0.52	0.2965	116.76	1.41	0.9477	29.52	22.51	0.8499	This work

Table 3. Thermodynamic functions (ΔG, ΔH and ΔS) for the adsorption process

Tem. K	1000/T	K_{eq}	ln K_{eq}	ΔG (kJ mol^{-1} K^{-1})	ΔH (kJ mol^{-1} K^{-1})	ΔS (J mol^{-1} K^{-1})
298	3.35	248.71	5.51	-13.66	59.17	-244.43
318	3.14	1270.02	7.14	-18.89	59.17	-245.50
338	2.95	4177.02	8.33	-23.42	59.17	-244.39
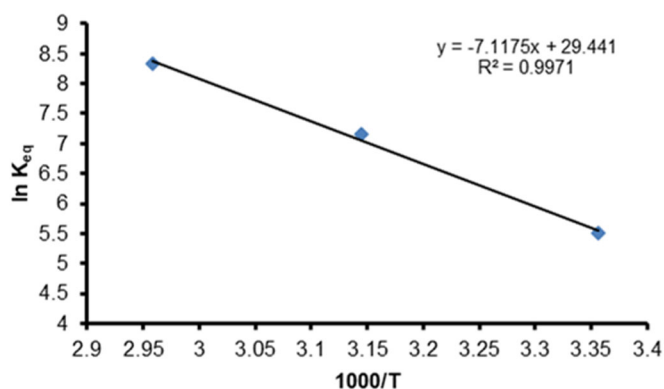
Fig 13. Calculation of ΔH for adsorption of MGO dye over the synthesized material by plotting of ln K_{eq} against 1000/T

change in entropy showed a change from a positive value but decreasing state with increasing temperature, this may be due to the disturbance of the water molecules around the dye [34-35].

$$\ln K_{eq} = \frac{-RH}{T} + con. \qquad (6)$$

$$K_{eq} = \frac{Q_e m}{C_e V} \qquad (7)$$

Substitute of Eq. (2) in Eq. (7):

$$K_{eq} = \frac{C_0 - C_e}{C_e} \qquad (8)$$

$$\text{Slope} = -R\Delta H \qquad (9)$$

$$\Delta G = -RT \ln K_{eq} \qquad (10)$$

$$\Delta S = \frac{\Delta G - \Delta H}{T} \qquad (11)$$

From the Isothermal models in Table 2 and thermodynamic values in Table 3, the removal mechanism of MGO dye was physical absorption because ΔG was negative as well. The isothermal models were not identical to the Langmuir model [36-37].

■ CONCLUSION

The present study involved the synthesis of a new spinel oxide nanocomposite successfully ($CuCo_2O_4/MgO$). The type of prepared composite was a spinel structure with a nanoparticles range. It showed high efficiency for the removal of MGO dye from its aqueous solutions, which was around 98%. Removal of MGO dye was conducted effectively using small quantities of adsorbent surface weight between 0.0025–0.015 g and dye concentration 5 mg L^{-1}.

■ ACKNOWLEDGMENTS

■ REFERENCES

[1] Farag, N.M., Deyab, M.A., El-naggar, A.M., Aldhafiri, A.M., Mohamed, M.B., and Heiba, Z.K., 2021, Exploring the functional properties of $CuCo_2O_4/CuS$ nanocomposite as improved

material for supercapacitor electrode, *J. Mater. Res. Technol.*, 10, 1415–1426.

[2] Qiao, X., Geng, W., Sun, Y., Zheng, D., Yang, Y., Meng, J., He, J., Bi, K., Cui, M., and Chou, X., 2021, Robust in-plane polarization switching in epitaxial $BiFeO_3$ films, *J. Alloys Compd.*, 852, 156988.

[3] Mohamad, E.J., 2015, Comparative Study to Synthesis and Characterization the Catalyst Ni_3O_4-Co_3O_4-Al_2O_3 and Usage in Photooxidation and Adsorption of Removal of Reactive Yellow145 and Bismarck Brown G Dyes, *Thesis*, University of Babylon, Iraq.

[4] Sun, J., Xu, C., and Chen, H., 2021, A review on the synthesis of $CuCo_2O_4$-based electrode materials and their applications in supercapacitors, *J. Materiomics*, 7 (1), 98–126.

[5] Al-samaray, H.S., 2018, Study the Removal of Celestine Blue Dye from Their Aqueous Solutions by Adsorption over the Mixed Oxide NiO-MgO Pure and Doped, *Thesis*, University of Babylon, Iraq.

[6] Dhara, K., and Debiprosad, R.M., 2019, Review on nanomaterials-enabled electrochemical sensors for ascorbic acid detection, *Anal. Biochem.*, 586, 113415.

[7] Ismael, H.A., Mohammad, E.J., Atiyah, A.J., Kadhim, S.H., and Kahdum, K.J., 2021, Synthesis and characteristic study of composite zinc oxide and functionalized activated carbon with investigation of its adsorption ability: A kinetic study, *IOP Conf. Ser.: Earth Environ. Sci.*, 722, 012007.

[8] Ahmadian, A., Bilal, M., Khan, M.A., and Asjad, M.I., 2020, Numerical analysis of thermal conductive hybrid nanofluid flow over the surface of a wavy spinning disk, *Sci. Rep.*, 10 (1), 18776.

[9] Kadhim, N.J., Mousa, S.A., Muhammed, E.A., and Farhan, A.M., 2020, A comparative study of the adsorption of crystal violet dye from aqueous solution on rice husk and charcoal, *Baghdad Sci. J.*, 17 (1), 295–304.

[10] Hussein, Z.A., Alazawy, R.A., and Haddawi, S.M., 2020, Adsorption of 2,6-dichlorophenol-indophenol sodium dihydrate salt from aqueous solutions using nano magnesium oxide; A thermodynamic study, *Egypt. J. Chem.*, 63 (10), 4157–4161.

[11] Al-Abadi, S.I., Al-Da'Amy, M.A., and Kareem, E.T., 2021, Thermodynamic study for removing of crystal violet dye on Iraqi porcelanite rocks powder, *IOP Conf. Ser.: Earth Environ. Sci.*, 790, 012055.

[12] Arora, C., Kumar, P., Soni, S., Mittal, J., Mittal, A., and Singh, B., 2020, Efficient removal of malachite green dye from aqueous solution using *Curcuma caesia* based activated carbon, *Desalin. Water Treat.*, 195, 341–352.

[13] Sharma, G., ALOthman, Z.A., Kumar, A., Sharma, S., Ponnusamy, S.K., and Naushad, M., 2017, Fabrication and characterization of a nanocomposite hydrogel for combined photocatalytic degradation of a mixture of malachite green and fast green dye, *Nanotechnol. Environ. Eng.*, 2 (1), 4.

[14] Ali, L.A.M., Farhood, A.S., and Ali, F.F., 2017, Technique of batch adsorption for the elimination of (malachite green) dye from industrial waste water by exploitation walnut shells as sorbent, *Indones. J. Chem.*, 17 (2), 211–218.

[15] Janjua, M.R.S.A., 2019, Synthesis of Co_3O_4 nano aggregates by co-precipitation method and its catalytic and fuel additive applications, *Open Chem.*, 17 (1), 865–873.

[16] Thahy, R.R.A., 2018, Synthesis and Identification of $Co_3O_4 \cdot Fe_3O_4/M_xO_x, M_xO_{x+1}$ where (M= Ca, Mg, Al, Ce) Spinel Supported Catalyst and Using It Removal of Bismarck Brown G Dye, *Thesis*, University of Babylon, Iraq.

[17] Kadhim, S.H., Kadhim, A.A., Al-Da'amy, M.A., and Kadhim, S.H., 2023, Synthesis of $CuCo_2O_4$-MgO spinel composite as an adsorbent surface for removal of celestine blue B dye, *AIP Conf. Proc.*, 2830 (1), 070034.

[18] Hicham, A., Hussein, J., and Siba, H., 2022, Kinetic, isotherm and thermodynamic studies on the ciprofloxacin adsorption from aqueous solution using Aleppo bentonite, *Baghdad Sci. J.*, 19 (3), 680–692.

[19] AL-Khazali, N.A.Y., 2017, Study Removal Remazol Brilliant Blue and Malachite Green Dyes from Aqueous Solutions Using Iraqi Porcelanite Rocks and Modified, *Thesis*, University of Kerbala, Iraq.

[20] Farhan, A.M., Zaghair, A.M., and Abdullah, H.I., 2022, Adsorption study of Rhodamine–B dye on plant (citrus leaves), *Baghdad Sci. J.*, 19 (4), 838–847.

[21] Das, A.K., Kim, N.H., Lee, S.H., Sohn, Y., and Lee, J.H., 2018, Facile synthesis of $CuCo_2O_4$ composite octahedrons for high performance supercapacitor application, *Composites, Part B*, 150, 269–276.

[22] Devaraja, P.B., Avadhani, D.N., Prashantha, S.C., Nagabhushana, H., Sharma, S.C., Nagabhushana, B.M., and Nagaswarupa, H.P., 2014, Synthesis, structural and luminescence studies of magnesium oxide nanopowder, *Spectrochim. Acta, Part A*, 118, 847–851.

[23] Sudha, V., Annadurai, K., Kumar, S.M.S., and Thangamuthu, R., 2019, $CuCo_2O_4$ Nanobricks as electrode for enhanced electrochemical determination of hydroxylamine, *Ionics*, 25 (10), 5023–5034.

[24] Petrov, K., Krezhov, K., and Konstantinov, P., 1989, Neutron diffraction study of the cationic distribution in $Cu_xCo_{3-x}O_4$ $(0<x\leqslant1.0)$ spinels prepared by thermal decomposition of layered hydroxide nitrate precursors, *J. Phys. Chem. Solids*, 50 (6), 577–581.

[25] Dana, J.D., 2022, *A System of Mineralogy*, Wiley, New Jersey, US.

[26] Helmy, Q., Notodarmojo, S., Aruan, I.A., and Apriliawati, R., 2017, Removal of color and chemical oxygen demand from textile wastewater using advanced oxydation process (AOPs), *IPTEK J. Proc. Ser.*, 3 (6), 474–481.

[27] Bonilla-Petriciolet, A., Mendoza-Castillo, D.I., and Reynel-Ávila, H.E., 2017, *Adsorption Processes for Water Treatment and Purification*, Springer, Cham, Switzerland.

[28] Abdul-aziz Umar, S., and Gaya, U.I., 2019, Optimised photocatalytic degradation of crystal violet over 1wt% MgO-ZnO composite catalyst, *J. Sci. Technol.*, 11 (1), 25–33.

[29] Obaid, S.A., 2020, Langmuir, Freundlich and Tamkin adsorption isotherms and kinetics for the removal Aartichoke Tournefortii straw from agricultural waste, *J Phys Conf Ser*, 1664, 012011.

[30] Chafat, A.H., Al-Da'amy, M.A., and Kareem, E.T., 2023, Iraqi porcelanite rocks for efficient removal of safranin dye from aqueous solution, *Baghdad Sci. J.*, 20 (2), 434–441.

[31] Shamsizadeh, A., Ghaedi, M., Ansari, A., Azizian, S., and Purkait, M.K., 2014, Tin oxide nanoparticle loaded on activated carbon as new adsorbent for efficient removal of malachite green-oxalate: Non-linear kinetics and isotherm study, *J. Mol. Liq.*, 195, 212–218.

[32] Mohamad Zaidi, N.A.H., Lim, L.B.L., and Usman, A., 2019, Enhancing adsorption of malachite green dye using base-modified *Artocarpus odoratissimus* leaves as adsorbents, *Environ. Technol. Innovation*, 13, 211–223.

[33] Brião, G.V., Jahn, S.L., Foletto, E.L., and Dotto, G.L., 2018, Highly efficient and reusable mesoporous zeolite synthetized from a biopolymer for cationic dyes adsorption, *Colloids Surf., A*, 556, 43–50.

[34] Hussein, Z.A., Haddawi, S.M., and Kadhim, A.A., 2019, Study of thermodynamic variables to adsorption of aldomete drug (methyldopa) from its water solution on the nano zinc oxide surface, *Int. J. Pharm. Qual. Assur.*, 10 (2), 315–321.

[35] Fouda, A., Hassan, S.E.D., Abdel-Rahman, M.A., Farag, M.M.S., Shehal-deen, A., Mohamed, A.A., Alsharif, S.M., Saied, E., Moghanim, S.A., and Azab, M.S., 2021, Catalytic degradation of wastewater from the textile and tannery industries by green synthesized hematite (α-Fe_2O_3) and magnesium oxide (MgO) nanoparticles, *Curr. Res. Biotechnol.*, 3, 29–41.

[36] Kadhim, S.H., Mgheer, T.H., Ismael, H.I., Kadem, K.J., Abbas, A.S., Atiyah, A.J., and Mohamad, I.J., 2019, Synthesis, characterization and catalytic activity of NiO-CoO-MgO nano-composite catalyst, *Indones. J. Chem.*, 19 (3), 675–683.

[37] Mustikaningrum, M., Cahyono, R.B., and Yuliansyah, A.T., 2022, Adsorption of methylene blue on nano-crystal cellulose of oil palm trunk: Kinetic and thermodynamic studies, *Indones. J. Chem.*, 22 (4), 953–964.